UNIVERSITY OF CALIFORNIA, SAN DIEGO

Laser Tweezers to Investigate Sperm Motility and Mitochondrial Respiration in Three Vertebrate Species

A thesis submitted in partial satisfaction of the requirements for the degree Master of Science

in

Bioengineering

by

Timothy Jerome Chen

Committee in charge:

Professor Michael W. Berns, Chair
Professor Shu Chien, Co-Chair
Professor Eric Lauga

2010

The thesis of Timothy Jerome Chen is approved, and it is acceptable in quality and form for publication on microfilm and electronically:

_____

_____
Co-Chair

_____
Chair

University of California, San Diego

2010

For my parents, Annie and David Chen, and my siblings,

Angela, Justin, and Christopher.

Table of Contents

List of Tables

List of Figures

Abbreviations and Symbols

Abbreviations

BSA: Bovine Serum Albumin

BWW: Biggers, Whittens, and Whittingham

CASA: Computer Assisted Sperm Analysis

CCCP: Carbonyl cyanide m-chloro phenyl hydrazone

$DiOC_6(3)$: 3,3'-dihexyloxacarbocyanine iodide

HTF: Human Tubal Fluid

Pesc: escape laser power, mW

SSS: Serum Substitute Supplement

VCL: curvilinear velocity, μm/second

Symbols

c – speed of light in media with given index of refraction

F – swimming force

μm – micron

mW – milliWatts

P – laser power

pN – picoNewton

Q – geometrically determined trapping efficiency parameter

Acknowledgements

I would like to acknowledge Professor Michael Berns for his continued support and guidance throughout my research and this thesis.

I would also like to acknowledge Dr. Linda Shi for her motivation and expertise.

I would also like to acknowledge the Wild Animal Park for supplying samples and help optimizing experimental procedures.

Chapter I, in part, is being prepared for submission for publication. Chen T., Shi L. Z., Zhu Q., Chandsawangbhuwana C., Berns M. W.

Chapter II, in part, is being prepared for submission for publication. Chen T., Shi L. Z., Zhu Q., Chandsawangbhuwana C., Berns M. W.

Chapter III, in part, is being prepared for submission for publication. Chen T., Shi L. Z., Zhu Q., Chandsawangbhuwana C., Berns M. W.

Chapter IV, in part, is being prepared for submission for publication. Chen T., Shi L. Z., Zhu Q., Chandsawangbhuwana C., Berns M. W.

Chapter V, in part, is being prepared for submission for publication. Chen T., Shi L. Z., Zhu Q., Chandsawangbhuwana C., Berns M. W.

Publications

Peer-Reviewed Publications

1. Shi L., Shao B., Chen T., Berns M. (2009). "Automatic annular laser trapping: a system for high-throughput sperm analysis and sorting". J Biophotonics. **2**(3) 167-77

Abstracts and Presentations

2. Chen T., Shi L. Z., Zhu Q., Chandsawangbhuwana C., Berns M. W. (2009). "Using laser tweezers and $DiOC_6(3)$, to measure sperm motilit." American Society of Cell Biology annual meeting. Poster presentation
3. Shi L. Z., Lauga E., Chen T., Berns M. W. (2010). "Solid boundaries decrease the propulsive force of swimming spermatozoa." American Society of Cell Biology annual meeting. Poster presentation

ABSTRACT OF THE THESIS

Laser Tweezers to Investigate Sperm Motility and Mitochondrial Respiration in Three Vertebrate Species

by

Timothy Jerome Chen

Master of Science in Bioengineering

University of California, San Diego, 2010

Professor Michael W. Berns, Chair
Professor Shu Chien, Co-Chair

The purpose of this study is to investigate how the mitochondrial membrane potential affects sperm motility using laser tweezers and the fluorescent probe, $DiOC_6(3)$. A 1064 nm Nd:YVO4 continuous wave laser was used to trap motile sperm at a power of about 450 mW in the focused trap spot. Using customized tracking software, the curvilinear velocity (VCL) and the escape force (Pesc) from the laser tweezers were measured. Human (*Homo sapiens*), dog (*Canis lupis familiaris*), and drill (*Mandrillus lecuophaeus*) sperm were labeled with the fluorescent dye $DiOC_6(3)$ to measure membrane potential in the mitochondria-rich sperm midpiece. The VCL

was measured frame by frame before trapping, and the fluorescence was measured before and during trapping. Fluorescence intensity of the dye-treated sperm was compared to unlabeled sperm. Controls were performed to verify that the $DiOC_6(3)$ does not affect sperm motility. Carbonyl cyanide *m*-chlorophenylhydrazone (CCCP) was used to inhibit mitochondrial respiration and cause a loss of fluorescence.

The results show that $DiOC_6(3)$ has no effect on the VCL and Pesc of the sperm even though there was a marked reduction in dye fluorescence when the CCCP was applied. Drill sperm exhibited a drop in VCL upon addition of CCCP, indicating a potential reliance on both glycolysis and aerobic respiration for motility. These results confirm that aerobic mitochondrial respiration is not the primary driving force for motility in human and dog sperm, but may be important for some primate species. $DiOC_6(3)$ was also proven to be an effective dye to study sperm mitochondrial energetics.

I. Introduction

1.1 Significance

Sperm motility is a valuable marker of sperm health and a good indicator of ability to properly capacitate and eventually fertilize an egg. The ability to evaluate sperm quality is critical for techniques such as in vitro fertilization (IVF), particularly when dealing with the reproduction of endangered animals. Understanding the mechanics and energetics of sperm motility also may provide useful information for future contraceptives (Amory, 2007); sperm with disabled or compromised motility will not be able to cross the "blood-testes" barrier, thus severely affecting its ability to reach the egg. Artificial insemination has proven to be vital for animal reproduction, particularly endangered species (Durrant, 2009). In order for successful insemination, high quality and quantity of sperm are necessary. Analysis of motility parameters can help answer the question of quality. Good motility analysis is also important when developing cryopreservation techniques, and addresses concerns of preserving human and animal semen for future fertilization. The fertilization ability of sperm may be indicated by the motility pre- and post-thaw (Wolf and Patton, 1989). Mahutte found that the best indicator for failed fertilization was the percentage of motile sperm on the day of sperm retrieval (Mahutte and Arici, 2003).

Curvilinear velocity (VCL) provides a key parameter for comparison of sperm between species or within a given species. A second parameter, sperm swimming force, has been measured with the aid of laser tweezers (Nascimento et al, 2006). This offers a relatively new parameter to help predict sperm fertilization ability. Sperm

motility is dependent on: (1) temperature – warmer temperatures lead to higher velocities, (2) depth in the chamber – determines amount of room for tail movement; (3) elapsed time – motility decreased over time at warm temperatures; and (4) rate of data acquisition -more points captured increases accuracy of measurement (Milligan et al, 1978). In this thesis, an automatic tracking software is used to accurately acquire data, while controlling for temperature and chamber depth. Experiments are performed in Rose chambers with a consistent chamber depth and temperatures.

1.2 Sperm Structure

The basic sperm structure consists of a head, midpiece, and tail. The head has very little cytoplasm and minimal organelles (Schmidt-Rhaesa, 1995), favoring a dense amount of genetic material and the acrosome. The acrosome, which tends to be at the tip of the head, contains enzymes to help the sperm penetrate the egg. The midpiece sits below the head and consists of a mitochondrial sheath and exceptionally stable outer membranes (Cummins, 2009). It is the site of mitochondrial respiration, supplying ATP for motility and other functions. The size of the midpiece and amount of mitochondria varies greatly among different species, reflecting different needs with regard to fertilization (Favard & Andre, 1970). The tail, or flagellum, is the means of motility that allows the sperm to reach the ovum for fertilization. Velocity is a function of wave frequency and amplitude of the tail beating (Bishop, 1962), both parameters of which depend on flagellum length and stiffness. When hyperactivation occurs in preparation for fertilization, the tail's amplitude becomes larger and more

asymmetrical (Yanagimachi, 1994). This change in beat pattern is in response to a need for an increase in force to help navigate the more viscous female tract.

The huge variety of sperm swimming environments has resulted in an evolution of many sperm types, including variations between head shape, head size, midpiece size, tail length, and energetics. Midpiece size does not necessarily equate to higher velocity or fertilization success. For example the red deer's long midpiece did not correlate with faster speeds (Malo et al, 2006). Malo also observed that elongated heads and relatively larger tail lengths correlated with faster velocities. On the other hand, Anderson observed a larger midpiece in primate species with greater sperm competition (Anderson and Dixson, 2002). Aside from sperm hydrodynamics and energetics, evolutionary need may play a role in motility parameters. A species that undergoes internal fertilization instead of external fertilization will have different energy requirements. Sperm in internal fertilization interacts with the uterus and oviduct to fertilize usually a small number of ova (Hancock, 1953). External fertilization, which many aquatic species undergo, is characterized by release of sperm into the environment with a high number of ova being fertilized. Depending on factors in each fertilization type, sperm may rely on both glycolysis (anaerobic) and oxidative phosphorylaton (aerobic) respiration, or just one of the two (Bedford and Hoskins, 1990). Human, which relies heavily on glycolysis, (Nascimento et al, 2008) has relatively few mitochondria, which have been shown to be more important for sperm hyperactivation, but not normal motility (Bedford and Hoskins, 1990).

Individual males also experience variation in sperm size and quality (Ward and Hauschteck-Jungen, 1993). The reason for varying sperm quality may lie in energy

efficiency. Sperm quality includes parameters such as motility, head shape, and the presence of any deformities. Rather than creating a small amount of very high quality sperm, males produce sperm ranging in quality, and the poor quality sperm will be selected out by the female reproductive tract (Parker and Partridge, 1998). When there is competition between males, sperm count is an important selection factor; when competition is small, then there is less pressure for high quality sperm (Bauer and Breed, 2006). Age also plays a role, as somatic mutations affecting sperm number and quality increase with age (Hansen and Price 1995). Within an individual male, sperm length is the one of the primary consistent characteristics, and velocity and percentage of live sperm important variable characteristics (Morrow and Gage, 2001b). In this thesis, sperm from a small group of males are used, but the collection dates vary.

The midpiece and its associated mitochondria are strong indicators of fertilization capability (Gallon et al, 2006). Gallon found that high mitochondrial membrane potential represented a healthy, normal, motile population of sperm with functional acrosomes and that membrane potential is a good predictor of fertilizing capability. Oxidative phosphorylation produces the majority of ATP when glucose is processed, but the means of transporting ATP along the long length of the flagellum for movement is still in debate. It is established that some sperm, such as human, require active glycolysis for full motility and hyperactivation (Williams and Ford, 2001). When glucose is not present, glycolysis-dependent sperm are still motile. Enzymes for gluconeogenesis have been found in dogs (Albarracin, 2004), indicating a possible pathway for continued glucose production for motility. Ford believes that gluconeogenesis is not the explanation, and that energy carriers such as adenylate

kinase may be the link (Ford, 2006). High activities adenylate kinase have been found in mammalian sperm (Schoff et al, 1989), but further research is required.

1.3 Ratiometric Dyes

There are many available chemical probes to measure mitochondrial activity. The most common means is to measure membrane potential, but protein and antibody binding to mitochondrial proteins is also utilized (Probes for Mitochondria, Invitrogen). Membrane potential dyes include carbocyanines ($DiOC_2(3)$, $DiOC_6(3)$, rhomadines (TMRE), JC-1, and rosamines (CMX-Ros). JC-1 has proven to be an effective dye for studying mitochondria in various systems, such as apoptosis (Salvioli et al, 1997). JC-1 is also the most commonly used dye for sperm studies; for example it has been used in rat (Gravance et al, 2001), and human (Marchetti et al, 2004). Marchetti found that although JC-1 may be effective, CMX-Ros, TMRE, and $DiOC_6(3)$ are also good dyes to study sperm energetics. Carbocyanine dyes, such as $DiOC_6(3)$ or $DiOC_2(3)$, have increasingly been used for mitochondrial studies in the past few years. $DiOC_2(3)$, a ratiometric dye, is not commonly used in sperm, which raises concerns of the repeatability of experimental results with other dyes. Nascimento used $DiOC_2(3)$ to demonstrate that glycolysis is the dominant process for motility for human and dog sperm (Nascimento, 2008).

This thesis will demonstrate that a non-ratiometric, carbocyanine dye, $DiOC_6(3)$, is a viable for investigating sperm motility. Compared to $DiOC_2(3)$, $DiOC_6(3)$ emits only one fluorescent wavelength, which opens up the future possibility of pairing other dyes with $DiOC_6(3)$. This dye has been found to successfully integrate

into mouse sperm (Breed and Sarafis, 1995), the endoplasmic reticulum and mitochondria at high concentrations (Sabnis et al, 1997), and human sperm (Gallon, 2006).

Inhibition of oxidative phosphorylation, or aerobic respiration, can be achieved with a variety of substances. Rotenone, antimycin A, and cyanide are commonly used, but affect various parts of the electron transport chain. Carbonyl cyanide m-chloro phenyl hydrazone (CCCP) is an inhibitor that works by disrupting the membrane potential and discharging the H^+ gradient in the mitochondria (Alvarado, 1998). Successful integration of CCCP would directly attack the source of $DiOC_6(3)$ fluorescence, resulting in a decrease or complete inhibition of fluorescence.

1.4 Scope

Chapter 2 introduces the theory behind optical trapping and how it is used. Chapter 3 describes the methods and materials, including the laser trapping system, the process of evaluating sperm motility and energetics. Real-time Automated Tracking and Trapping (RATTS) is discussed in detail, and the preliminary dye evaluation is given. In chapter 4, the results of controls and experiments on sperm are reported: human, dog, and drill sperm motility and energetics are studied. In chapter 5, the results and future work are discussed, focusing on the source of energy for sperm and validity of using $DiOC_6(3)$ as a sperm mitochondrial dye. Future experiments to further test the abilities of the dye, investigate the effect of midpiece size, and other experiments are discussed.

Chapter I, in part, is being prepared for submission for publication. Chen T., Shi L. Z., Zhu Q., Chandsawangbhuwana C., Berns M. W.

References

Albarracin J. L. (2004). Gluconeogeneis-linked glycogen metabolism is important in the achievement of in vitro capacitation of dog spermatozoa in a medium without glucose. *Biol of Reprod*. **71**, 1437-1445

Alvarado F., Vasseur M. (1998). Direct inhibitory effect of CCCP on the Cl^--H^+ symporter of the guinea pig ileal brush border membrane. *Am J Physiol Cell Physiol*. **274**, C481-C491

Amory J. K. (2007). Inhibiting sperm motility for male contraception: will the sperm tail be its "Achilles Heel." *Molecular Interventions*. **7**(2), 68-70.

Anderson M. J., Dixson A. F. (2002). Sperm competition: motility and the midpiece in primates. *Nature*. **16**(6880), 496

Bauer M., Breed W. G. (2006). Variation of sperm head shape and tail length in a species of Australian hydromyine rodent: the spinifex hopping mouse, Notomys alexis. *Reprod Fertil Dev*. **18**(7), 797-805

Bedford J. M., Hoskins D. D. (1990). The mammalian spermatozoon: morphology, biochemistry, and physiology. In *Marshall's Physiology of Reproduction* **2**, 379-568, Springer

Bishop W. (1962) Sperm Motility. *Physiol Rev*. **42**, 1-59

Breed W. G., Sarafis V. (1995). The fluorescent dye 3, 3' dihexyloxacarbocyanine iodide selectively stains the midpiece and apical region of the heads of murid rodent spermatozoa. *Biotechnic & Histochem.* **70**(6): 267-283

Cummins J. (2009). Sperm motility and energetics. In *Sperm Biology: An Evolutionary Perspective*. 185-206. Elsevier

Durrant B. S. (2009). The importance and potential of artificial insemination in CANDES (companion animals, non-domestic, endangered species). *Theriogenology*. **71**(1), 113-122.

Favard P. and Andre J. (1970) in *Comparative Spermatology*, ed. B. Bacetti, (Academic Press, New York), 415-429

Ford W. C. L. (2006). Glycolysis and sperm motility: does a spoonful of sugar help the flagellum go round? *Human Reprod Update*. **12**(3), 269-274

Gallon F., Marchetti C., Jouy N., Marchetti P. (2006). The functionality of mitochondria differentiates human spermatozoa with high and low fertilizing capacity. *Fertil Steril.* **86**(5), 1526-1530

Gravance C. G., Garner D. L., Miller M. G., Berger T (2001). Fluorescent probes and flow cytometry to assess rat sperm integrity and mitochondrial function. *Reprod Toxicol.* **15**(1), 5-10

Hancock J. L. (1953). The spermatozoa of sterile bulls. *J. Exp. Biol*. **30**, 50-56

Hansen T.F., Price D. K. (1995). Good genes and old age: do old males provide superior genes?. *Journal of Evolutionary Biology*. **8**, 759–778

Marchetti C., Jouy N., Leroy-Martin B., Defossez A., Formstecher P., Marchetti P. (2004). Comparison of four fluorochromes for the detection of the inner mitochondrial membrane potential in human spermatozoa and their correlation with sperm motility. *Human Reprod*. **19**(10), 2267-2276

Mahutte N. G., Arici A. (2003). Failed fertilization: is it predictable? *Curr Opin Obstet Gynecol*. **15,** 211–218

Malo A. F., Gomendio M, Garde J, Lang-Lenton B., Soler A. J., Roldan E. R. (2006). Sperm design and sperm function. *Biol Lett*. **2**(2), 246-249

Milligan M. P., Harris S. J., Dennis K. J. (1978). The effect of temperature on the velocity of human spermatozoa as measured by time lapse photography. *Fertil Steril.* **30**(5), 592-594

Morrow E.H., Gage M. J. G. (2001). Consistent significant variation between individual males in spermatozoal morphometry. *J. Zool*. **254**, 147-153

Nascimento J. M., Botvinick E. L., Shi L. Z., Durrant B., Berns M. W. (2006). Analysis of sperm motility using optical tweezers. *J Biomed Opt*. **11**(4):044001

Nascimento J. M., Shi L. Z., Tam J., Chandsawangbhuwana C., Durrant B., Botvinick E. L., Berns M. W. (2008). Comparison of glycolysis and oxidative phosphorylation as energy sources for mammalian sperm motility, using the combination of fluorescence imaging, laser tweezers, and real-time automated tracking and trapping. *J. Cell. Physiol.* **217**, 745-751

Parker G. A., Partridge L. (1998). Sexual conflict and speciation. *Philos Trans R Soc Lond B Biol Sci.* **353**(1366), 261-274

Sabnis R. W., Deligeorgiev T. G., Jachak M. N., Dalvi T. S. (1997). $DiOC_6(3)$: a useful dye for staining the endoplasmic reticulum. *Biotechn & Histochem*. **72**(5), 253-258

Salvioli S., Ardizzoni A., Franceschi C., Cossarizza A. JC-1, but not $DiOC_6(3)$ or rhodamine 123 is a reliable fluorescent probe to assess delta psi changes in intact cells: implications for studies on mitochondrial functionality during apoptosis. *FEBS Lett.* **411**(1), 77-82

Schmidt-Rhaesa A. (2007). Gametes (Spermatozoa). *Evolution of Organ Systems*. 262-292

Schoff P. K., Cheetham J., Lardy H. A. (1989). Adenylate kinase activity in ejaculated bovine sperm flagella. *J Biol Chem*. **264**(11), 6086-6091

Ward P.I., Hauschteck-Jungen E. (1993). Variation in sperm length in the yellow dung fly *Scathophaga stercoraria* (L). *Journal of Insect Physiology*. **39**, 545–547

Williams K. M., Ford W. C. (2001). The role of glucose in supporting motility and capacitation in human spermatozoa. *J Androl*. **22**(4), 680-695

Wolf D. P., Patton P. E. (1989). Sperm Cryopreservation: state of the art. *J In Vitro Fert Embryo Transf*. **6**(6), 325-327

Yanagimachi R. (1994). Fertility of the mammalian spermatozoa: its development and relativity. *Zygote*. **2**(4), 371-372.

II. Optical Trapping

2.1 Introduction

Optical traps (tweezers) are tools to micromanipulate cells and determine cell motile force (Berns et al, 1998). Tweezers can hold onto particles or cells, and move them to different locations. Optical tweezers cause relatively little damage and minimally affect cell reproduction (Ashkin, 1991). The strength of the laser can also be attenuated over time, thus allowing the cell to swim away eventually, permitting calculation of the swimming force. The equation for swimming force is

$$F = Q \times P/c$$

where Q is trapping efficiency parameter dependent on the laser and optical properties of the cell, P is the power the cell escaped from the trap, and c is the speed of light in the medium (Konig, 2000). The ideal optical tweezers wavelengths for trapping sperm fall between 800-1064 nm (Konig, 1996) and have been used to successfully measure sperm swimming force (Patrizio et al, 2000; Nascimento et al. 2006). Using laser tweezers, Patrizio found that pentoxyifylline dramatically increases in the swimming force of sperm and Nascimento studied sperm competition (Nascimento et al. 2008a) and energetics (Nascimento et al, 2008b). Shi manipulated the laser into an axicon ring trap to perform high throughput sorting and motility analysis (Shi et al, 2009).

2.2 Theory of optical trapping

The principle of optical trapping relies on the momentum of photons. The laser is focused to near a diffraction-limited spot which passes through a relatively

transparent particle. The change in index of refraction after the photons hit the particle causes a shift in momentum, and the generation of gradient and scattering forces on the particle. The scattering force, caused by reflection and stray refraction of the light, must be overcome by the gradient force to stabilize the trap. The change in momentum affects the ray optics of the light; each ray has its own direction, intensity, polarization that will hit the particle (Ashkin, 1992). Since particles tend to have a larger index of refraction, the light bends towards a specific point. The gradient and scattering forces act as a dipole-electric field (Ashkin 1992), with the scattering force acting in the direction of the light and the gradient force drawing the particle to the new focus point created by the light refraction (Figure 2.1).

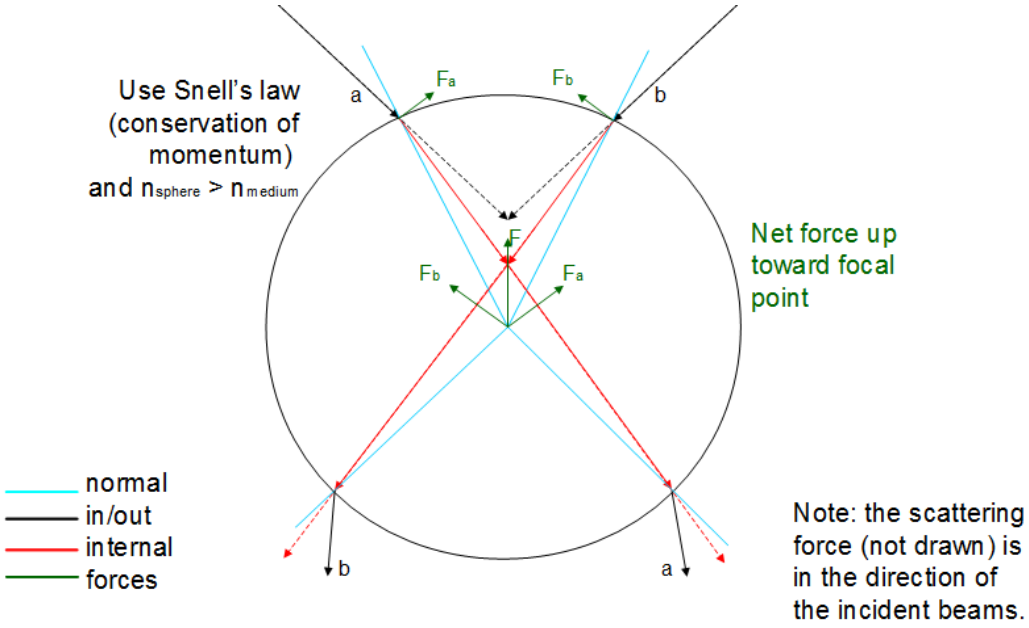

Figure 2.1: Shows how the light, coming from the top, refracts upon hitting the particle. The focus of the laser is shifted to point F and will successfully trap sperm if the trapping force is greater than the swimming force of the sperm (Picture courtesy of Jaclyn Nascimento).

The laser used in this thesis is a Nd:YVO_4 continuous wave 1064nm wavelength laser (Spectra Physics, Model BL-106C, Mountain View, CA). Optical tweezers strength is proportional to laser intensity (Neuman and Block, 2004). The actual laser power after the traveling through the microscope, and objective lens is approximately 450 mW in the focal point.

Chapter II, in part, is being prepared for submission for publication. Chen T., Shi L. Z., Zhu Q., Chandsawangbhuwana C., Berns M. W.

References

Ashkin A. (1991). The study of cells by optical trapping and manipulation of living cells using infrared laser beams. *ASGSB Bull*. **4**(2), 133-146.

Ashkin A. (1992). Forces of a single-beam gradient laser trap on a dielectric sphere in the ray optics regime. *Biophys J.* **61**, 569-582.

Berns M.W., Tadir Y., Liang H., Tromberg B. (1998). Laser scissors and tweezers. *Methods Cell Biol.* **55**, 71-98

Konig K. (2000) Multiphoton microscopy in life sciences. J Microsc. **200**(Pt 2), 83-104

Konig K., Svaasand L., Liu Y., Sonek G., Patrizio P., Tadir Y., Berns M. W., Tromberg B. J. (1996). Determination of motility forces of human spermatozoa using an 800 nm optical trap. *Cell Mol Biol (Noisy-le-grand)* **42**(4), 501-509.

Nascimento, J. M., Botvinick, E. L., Shi, L. Z., Durrant, B., Berns, M. W. (2006). Analysis of sperm motility using optical tweezers. *J Biomed Opt*. 11(4):044001

Nascimento J. M, Shi L.Z., Meyers S., Gagneux P., Loskutoff N.M., Botvinick E.L., Berns M.W. (2008a). The use of optical tweezers to study sperm competition and motility in primates. *J R Soc Interface.* **5**, 297-302

Nascimento J. M., Shi L. Z., Tam J., Chandsawangbhuwana C., Durrant B., Botvinick E. L., Berns M. W. (2008b). Comparison of glycolysis and oxidative phosphorylation as energy sources for mammalian sperm motility, using the combination of fluorescence imaging, laser tweezers, and real-time automated tracking and trapping. *J Cell Physiol.* 217, 745-751

Neuman K. C., Block S. M. (2004). Optical trapping. *Rev Sci Instrum.* **75**(9), 2787-2809.

Patrizio P., Liu Y., Sonek G. J., Berns M. W., Tadir Y. (2000). Effect of pentoxyifylline on the intrinsic swimming forces of human sperm assessed by optical tweezers. *J Androl*. 21(5), 753-756.

Shi L., Shao B., Chen T., Berns M. (2009). Automatic annular laser trapping: a system for high-throughput sperm analysis and sorting. **2**(3), 167-177

III. Sperm Preparation and Data Collection

3.1 Introduction

This chapter outlines the primary materials and methods used to test $DiOC_6(3)$ on sperm. This includes the process of sperm collection and preparation, data collection and analysis, and dye interaction with the sperm. The semen samples were cryopreserved and thawed differently for each species, but followed a similar overall protocol. RATTS was used to control the necessary hardware to analyze the sperm samples. RATTS calculated the motility and energetics automatically, requiring the user to select the sperm and ensure proper tracking. The fluorescence intensity was analyzed via comparison with the background. Random sperm samples were studied in order to evaluate the effect of photobleaching.

3.2 Materials and Methods

3.2.1 Sample Collection and Preparation

Semen samples for human, dog, and drill were tested. Human samples were supplied by a local La Jolla fertility clinic. The samples was collected after 3 days of abstinence and added to 10 mL of Biggers, Whittens, and Whittingham (BWW), penicillin, and streptomycin. The samples were frozen according to a normal human freezing protocol (Ethics Committee of the American Fertility Society, 1986; DiMarzo et al, 1990; Serfini and Marrs, 1986). The samples were thawed, and centrifuged at 2000 rpm for ten minutes. The solution was decanted, mixed in Human Tubal Fluid (HTF) HEPES buffered with filtered 5% serum substitute supplement, centrifuged, and resuspended; this is considered a two-wash technique. For all sperm studies, a

final dilution of ~30,000 sperm per mL were loaded into Rose culture chambers (about .5 uL of sperm in 2.5 mL media), and mounted on the microscope.

Dog samples were taken from the epididymis by flushing the vas and collecting from the incised cauda epididymis. The sperm were suspended with Test-Yolk buffer, cooled for 30 minutes at 4ºC, supplemented with glycerol, and frozen over liquid nitrogen using methods perfected at the San Diego Zoo (Durrant et. al. 2000) . The samples, supplied by the San Diego Zoo/Wild Animal Park, were thawed at 37ºC, centrifuged at 2200 rpm for ten minutes, and decanted; this is considered a single-wash. The pellet was mixed with BWW+BSA (BWW + 1mg/mL of bovine serum albumin). Approximately 1 uL of sperm was diluted into 2.5 mL media, and loaded into Rose chambers for experimentation.

Drill samples were cryopreserved following a similar protocol to dog (Durrant et al, 1999). The samples were thawed and centrifuged at 2200 rpm for ten minutes and decanted. The pellet was mixed with Medium 199 (M199), and ~50 uL of sperm are diluted into 2.5 mL media, and loaded in Rose chambers.

3.2.2 Optical design

The tracking and trapping system uses a Nd:YVO_4 continuous wave 1064nm wavelength laser (Spectra Physics, Model BL-106C, Mountain View, CA) traveling through a series of lenses and mirrors (Figure 3.1) to enter a Zeiss Axiovert S100 microscope and a 40x, phase III, NA 1.3 oil immersion objective (Zeiss, Thornwood, NY). The laser is reflected by two mirrors that directs it towards the microscope and then passes through a mechanical shutter before entering the objective. A motorized

rotating polarizer allows for control of the laser power, and slowly attenuates the beam during sperm escape power measurements. The beam expanding lenses and focusing lens cause the collimated laser to fill the objective's back aperture with a maximum amount of energy in the laser trapping focal spot.

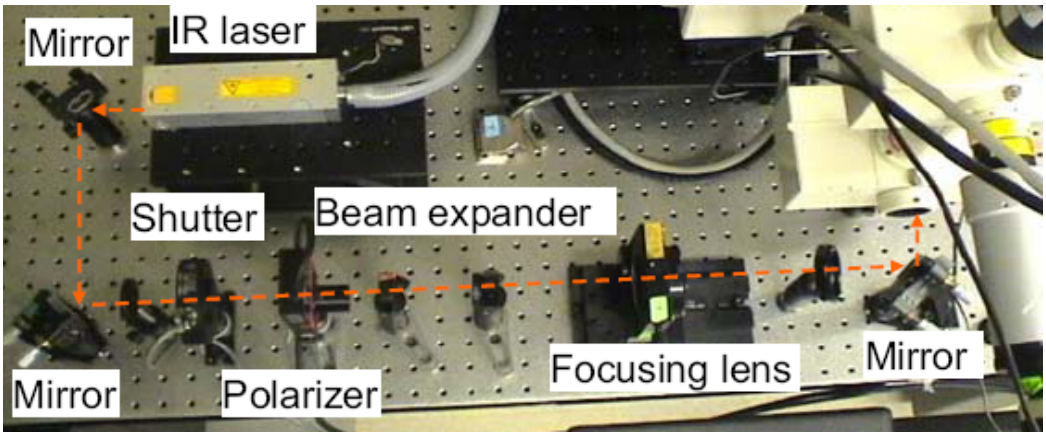

Figure 3.1: The laser path before it enters the microscope (Nascimento, 2008).

The microscope configuration permits collection of phase and fluorescence images (Figure 3.2). The laser passes through a dichroic (Figure 3.2, long-pass dichroic) filter that reflects visible light from the microscope optical system to the above-mounted camera systems. Before it hits the objective, a filter cube with a HQ 475/25 nm excitation filter and 505 nm dichroic allows for fluorescence activation of the specimen in the image plane. A Zeiss Fluor arc lamp provides the excitation light via epi-illumination through the microscope objective. The red filter above the image plane allows for separation of phase contrast (670 nm) and fluorescence (500-670 nm) images. These images are then reflected into the dual video camera optical system for separation into their respective parts. The dual video system attached to the top port of the first video adapter separates the phase information (reflects > 670nm) from the

fluorescence information (transmits 500-670 nm). The reflected phase information is collected by a charge coupled device (CCD) camera (Cohu model 7800, San Diego, CA) at 30 fps. The fluorescence information passes through a HQ 500/20 nm emission filter and is collected by a digital camera (Quantix 57, Roper Scientific Inc., Tuscon, AZ).

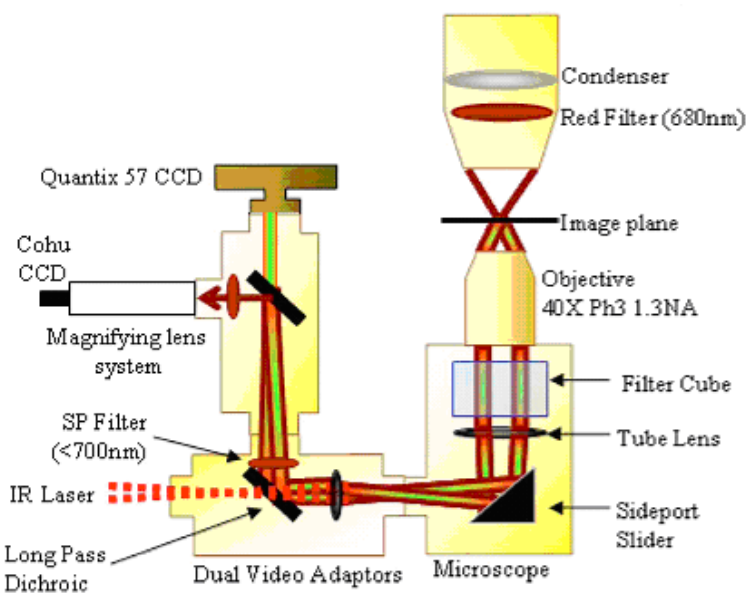

Figure 3.2: The path of the laser and visible light in the microscope. The laser travels to the image plane, while the image is broken up into two parts in the visible light spectrum and collected by two separate cameras.

3.2.3 Hardware and Software System

In early studies, the experimenter would have to constantly look at the sperm swimming patterns on the images captured by the CCD camera, manually move the joystick, which connects to the x-y microscope stage, to relocate the sperm-of-interest in the laser trap, and then depress the top button on the joystick connected to the mechanical shutter to turn on the laser trap. This was relatively easy for slow

swimming sperm and virtually impossible for faster (>100 um/sec) sperm. In addition, it was necessary to record the swimming velocity both before and after the sperm was trapped, and as will be seen in a later section, monitor the cellular respiration before, during, and after laser trapping. The solution to this problem was the development of a real-time automated tracking and trapping system (RATTS) that operates at video rate and provides remote robotic interfaces with the hardware.

In this thesis, RATTS has been modified to measure mitochondrial membrane potential (prior to, during, and after laser trapping) in conjunction with swimming speed and escape laser power of individual sperm. Figure 3.3 shows the system hardware diagram. The components in the upper-level system are indicated in the double-line box in Figure 3.3. The host computer contains an ASUS P5AD2 mother board, and two hard drives were connected through the motherboards' RAID level 0 controller. An image acquisition board in the host computer digitizes analog video signals. A 7344 motion controller is housed in a PXI chassis, which is controlled from the host PC, through a MXI-3 link connected with a fiber-optic cable. A MXI-3 PCI interface card in the host computer transmits/receives data to the MXI-3 PXI card in the PXI chassis through a bidirectional fiber-optic cable, thereby implementing a PCI-PCI bridge. A 4-axis stepper-motor driver connected to the motion controller drives the x-y stepper-motor stage of the microscope. Video signals from an RS-170 standard CCD camera are distributed to a TV monitor, a camcorder for recording, and an image acquisition board through a video distribution amplifier (not shown). A mechanical shutter in the laser path is controlled by a shutter driver through two lines of digital input–output from the motion controller. A rotary stepper motor mount housing a Glan

laser linear polarizer is controlled by the motion controller and stepper motor driver to modulate power in the laser trap. The lower-level system, shown in the single-line box in Figure 3.3, contains a Dell Socket 478 P4 planar. An image acquisition board is housed in the computer to digitize the camera signal from the Quantix camera. A data acquisition board is also housed in the computer to control the arc lamp shutter (placed in front of Zeiss Fluo Arc lamp) through a shutter driver. The dual-view system in front of the Quantix camera images two spectrally separated copies of the specimen plane onto the camera. The color channels are aligned prior to each experiment.

The real-time sperm tracking, automatic laser trapping, and ratiometric fluorescent image processing is custom coded in the LabView language. The RATTS interface for controlling the hardware is seen in Figure 3.4 (Shi et al., 2006). The operation of real-time tracking and automatic laser trapping is performed in the upper-level system. Fluorescent image acquisition, processing and storage are done in the lower-level system. The two computers are networked together over a gigabit TCP/IP cat5e crossover connection (not shown in Figure 3.3). Communication between the two systems is optimized with Labview's shared variables and VI server functions in which the lower-level system continuously polls the upper-level system for the next request. This polling method requires a minimal time for communication.

Using RATTS, sperm are tracked for extended durations before and after laser trap experiments. Motility measurements including VCL and the absolute position of the sperm relative to the cell chamber are calculated and written to the hard drive at video rates. Experimental throughput is increased over 30 times compared to off-line data analysis.

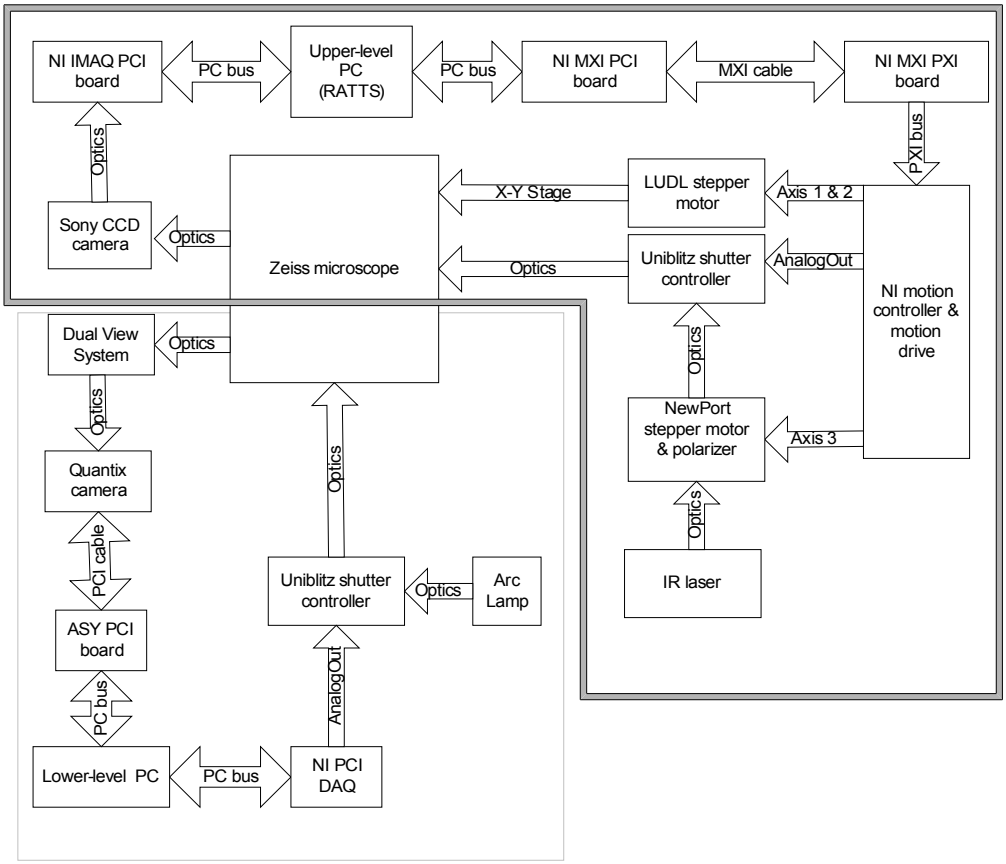

Figure 3.3: Hardware diagram of system to study sperm motility and energetics (Shi, et al., 2006). The upper-level system includes the components in the double-line box, and the lower-level system includes the components in the single-line box.

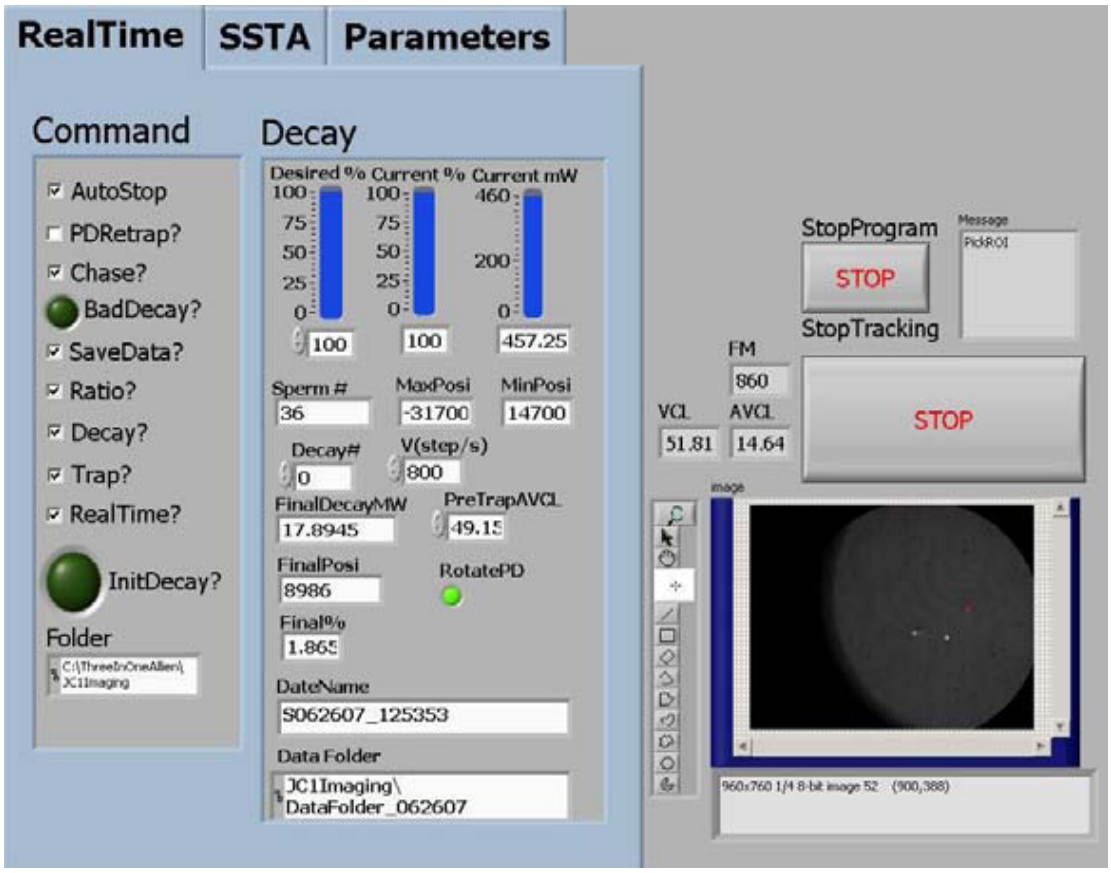

Figure 3.4: The primary interface for RATTS on Labview 9.0. It can control the laser shutter, the polarizer, and the cameras.

3.3 Testing $DiOC_6(3)$

The purpose of this section is to evaluate the effect $DiOC_6(3)$ has on sperm, and to determine its ideal concentration. The fluorescence of the untreated sperm is considered the baseline fluorescence. Fluorescence ratio was determined by finding the difference of measured fluorescence intensity of a sperm and the baseline fluorescence, and then dividing by baseline. A fluorescence value close to or at zero indicates little or no fluorescence, and a value greater than zero indicates noticeable fluorescence. Human sperm were evaluated at 30, 40, and 50 nM of dye exposure; the

dog sperm at 40 and 50 nM; and the drill at 10, 30, and 50 nM. Figure 3.5 presents fluorescence at ideal concentrations in human, dog, drill, mouse, and pig.

Figure 3.5: $DiOC_6(3)$ fluorescing in various species' sperm. Pig and mouse sperm are discussed in Appendix A. The concentration of $DiOC_6(3)$ is 40 nM for human and 50 nM for the other four species.

The dye was added after the sperm washing protocols and incubated at 37ºC for 20 minutes. Using the above fluorescence algorithm, fluorescence values were found at various concentration. The further the value from zero, the greater the fluorescence. Human had fluorescence of .25, .23, and .16 at 30, 40, and 50 nM, respectively. Dog was .23 and .21 at 40 nM and 50 nM. Drill was .03, .08, and 0.3 at 10, 30, and 50 nM. The experimental concentration chosen was 40 nM for human and 50 nM for dog and drill.

Photobleaching was not found to be a problem, as the fluorescence intensity did not change in sperm tracked for a long time while exposed to the arc lamp. Figure 3.6 shows a sample indicative of a normal sperm stained with $DiOC_6(3)$.

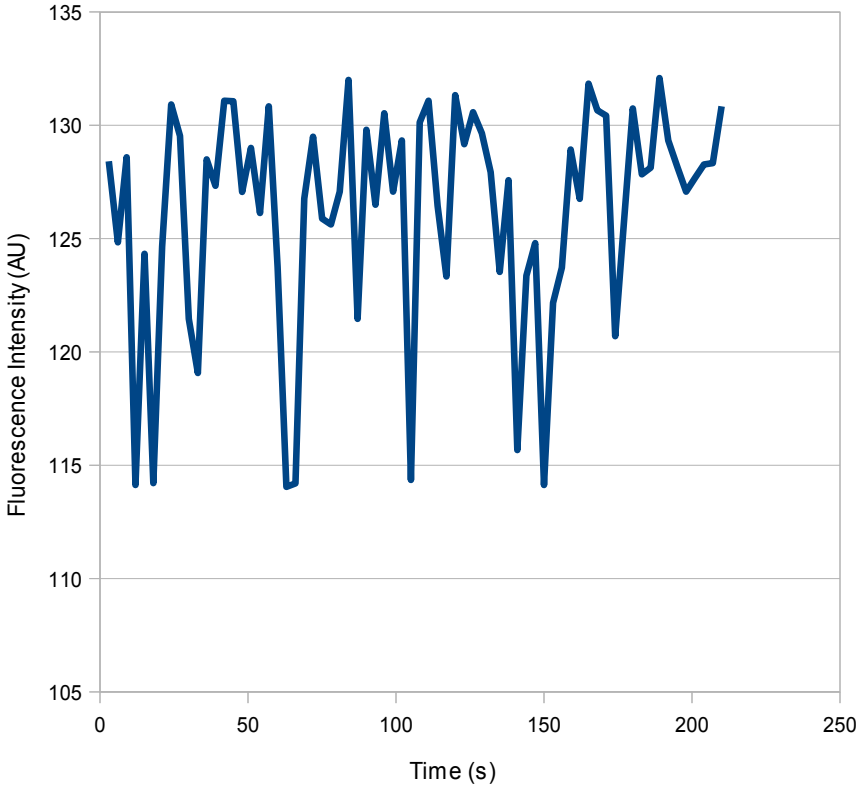

Figure 3.6: The fluorescence intensity (arbitrary units) versus time (seconds). The time span investigated is much longer than normal tracking of sperm and are thus exposed to much more arc-lamp. Despite slight variations in fluorescence intensity, the intensity did not appear to decrease over time.

In order to determine whether the dye was targeting the membrane potential of the mitochondria, CCCP was added after dye incubation (for the human and dog samples), or at the same time as the dye (drill samples). CCCP was added at 10 nM, a concentration similar to the amount used in neutrophils (Korchak et al, 1982), or slightly higher than what was used in human sperm (Guzman-Grenfell et al, 2000).

Chapter III, in part, is being prepared for submission for publication. Chen T., Shi L. Z., Zhu Q., Chandsawangbhuwana C., Berns M. W.

References

DiMarzo S. J., Huang J., Kennedy J. F., Villanueva B., Hebert S. A., Young P. E. (1990) Pregnancy rates with fresh versus computer-controlled cryopreserved semen for artificial insemination by donor in a private practice setting. *Am J Obstet Gynecol.* ***162****, 1483–1490*

Durrant B. S., Harper D., Amodeo A., Anderson A. (2000) Effect of extraction methods on cryopreservation of canine epididymal sperm. *Biology of Reproduction* 62(Suppl. 1): 144-145

Durrant B. S., Cammidge L., Wiley S., Carlsson I., Wesche P., Russ K. (1999). Cryopreservation of semen from the drill baboon. *Soc Study Reprod*.

Guzman-Grenfell A. M., Bonilla-Hernandez M. A., Gonzalez-Martinez M. T. (2000). Glucose induces a Na(+),K(+)-ATPase-dependent transient hyperpolarization in human sperm. I. Induction of changes in plasma membrane potential by the proton ionophore CCCP. Biochim Biophys Acta. **1464**(2), 188-198

Farrell P. B., Presicce G. A., Brockett C. C., Foote R. H. (1998). Quantification of bull sperm characteristics measured by computer-assisted sperm analysis (CASA) and the relationship to fertility. *Theriogenology.* **49**(4), 871-879

Kime D. E., Van Look K. J. W., McAllister B. G., Huyskens G., Rurangwa E., Ollevier F. (2001). Computer-assisted sperm analysis (CASA) as a tool for monitoring sperm quality in fish. *Comp Biochem and Physio Part C: Tox & Pharm*. **130**(4), 425-433.

Korchak H. M., Rich A. M., Wilkenfeld C., Rutherford L. E., Weissmann G. (1982) A carbocyanine dye, $DiOC_6(3)$, acts as a mitochondrial probe in human neutrophils. *Biochem and Biophys Research Communications*. **108**(4), 1495-1501

Mortimer D. (1994). *Practical laboratory andrology,* Oxford University Press, New York, NY.

Nascimento J. M., Shi L. Z., Tam J., Chandsawangbhuwana C., Durrant B., Botvinick E. L., Berns M. W. (2008b). Comparison of glycolysis and oxidative phosphorylation as energy sources for mammalian sperm motility, using the combination of fluorescence imaging, laser tweezers, and real-time automated tracking and trapping. *J. Cell. Physiol.* 217, 745-751

Serfini P., Marrs R. P. (1986). Computerized staged-freezing technique improves sperm survival and preserves penetration of zona-free hamster ova. *Fertil Steril.* **45**, 854-858.

Shi L. Z., Nascimento J., Chandsawangbhuwana C., Berns M. W, Botvinick E. L. (2006). Real-Time automated tracking and trapping system for sperm. *Microscopy Research and Techniques.* **69**, 894-902.

Kuo K. L., Tzeng W. L., Li P. C., Young S. T. (2000). Autostage sperm tracing system for semen evaluation. *Systems Biology in Reprod Medicine.* **44**(1), 29-39

Young S. T., Tzeng W. L., Kuo Y. L., Ksiao M. L., Chiang S. R. (1996). Real-time tracing of spermatozoa. *IEEE Eng in Med and Bio.* ***15***(6), 117-120.

IV. Results: Motility and energetics of mammalian sperm

4.1 Introduction

In this chapter, the motility and energetics of the sperm of three different mammalian species are compared. The species of interest are the human, dog, and drill. The protocol for sample preparation was outlined in Chapter 3.2.1. For each species, three different groups were tested: untreated sperm, sperm incubated in $DiOC_6(3)$, and sperm incubated in $DiOC_6(3)$ and the metabolic poison, CCCP. Since sperm populations do not have Gaussian distributions, the non-parametric Wilcoxon rank sum test was used to test for statistical significance (Donnelly et al, 2001). Each of the three groups were compared with each other: untreated vs. dye; untreated vs. dye and CCCP; dye vs. dye and CCCP. Fluorescence and VCL were graphed against each other to study the relationship between mitochondrial activity and sperm motility.

4.2 Results

4.2.1 Human

The VCL, escape force, and fluorescence ratio were averaged for each of the three species. Table 4.1 presents the results of human sperm, and Table 4.2 shows the statistical significance for each of the test groups. VCL and swimming force were found to be statistically equivalent. The addition of $DiOC_6(3)$ resulted in a clear increase in fluorescence, while the CCCP effectively reduced the fluorescence. The groups were also compared by box-plot in Figure 4.1. The measurements indicate that

the observed fluctuation in force is statistically insignificant. Despite large differences in their means, the medians are statistically similar.

Table 4.1: VCL, swimming force, and fluorescence ratio (calculation method outlined earlier) averages for human sperm. The number of samples collected are in the parenthesis next to each average. There is very little variation between VCL and some variation between swimming force. The addition of dye caused noticeable fluorescence, and CCCP eliminated the fluorescence.

	No Dye	Dye	CCCP + Dye
Human VCL (μm/sec)	82.13 (n=148)	84.58 (n=411)	82.65 (n=160)
Human Swimming Force (pN)	38.1 (n = 114)	26.2 (n=251)	31.0 (n=87)
Human Fluorescence Ratio (vs. No $DiOC_6(3)$)	-1.74×10^{-5} (n=65)	.202 (n=122)	.023 (n=78)

Table 4.2: There was no statistical significance between any of the three groups for VCL and swimming force. A value less than .05 indicates significance. The increase in fluorescence upon addition of $DiOC_6(3)$ was significant compared to the untreated sperm, and the depolarized CCCP-treated sperm.

	No Dye vs. Dye	No Dye vs. CCCP + Dye	Dye vs. CCCP + Dye
Human VCL	0.93	0.65	0.62
Human Swimming Force	0.34	0.06	0.32
Human Fluorescence	**2.37×10^{-29}**	**6.16×10^{-22}**	**9.85×10^{-33}**

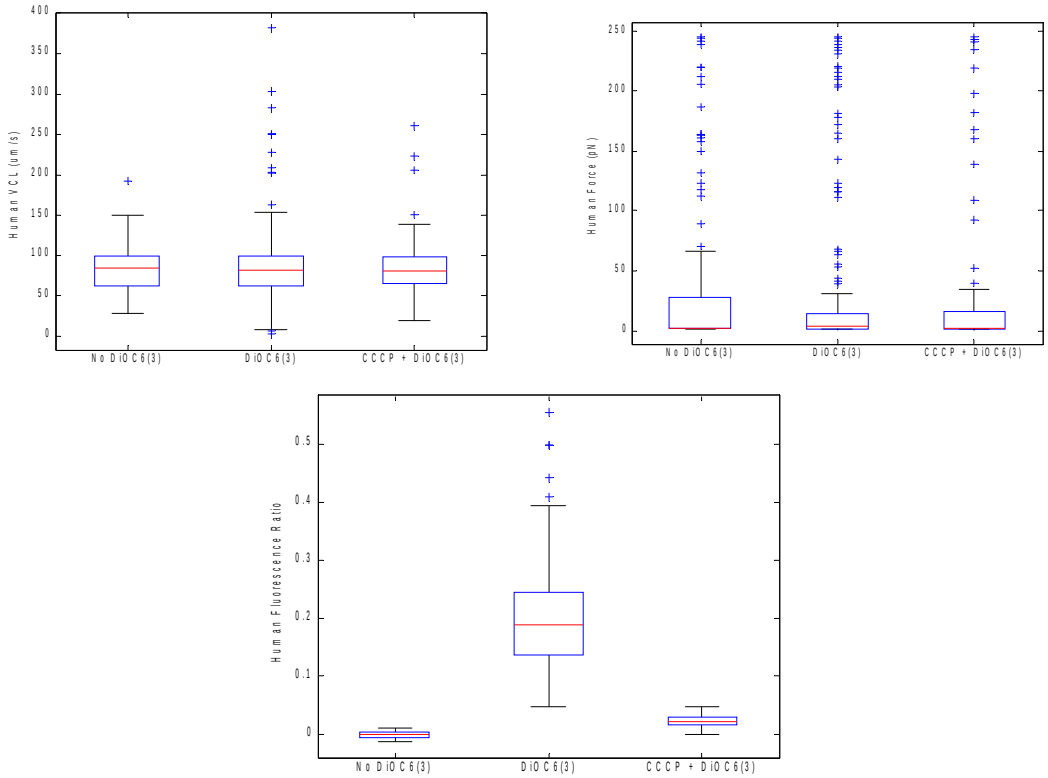

Figure 4.1: Boxplots for the three human sperm groups. The VCL for each of the groups are very similar in median and distribution. The swimming force had many outliers for each group, but a similar median. The dye group had a large range of fluorescence, all of them higher than the no dye and dye + CCCP groups, which had a very small range.

Human sperm were also washed and prepared in no-glucose BWW media. Wash and incubation in media with no glucose allows for investigation of sperm activity when glucose is not available, thus forcing aerobic respiration to supply the energy (ATP) for motility. The resulting VCL was only 44.15 um/s (n = 22). When CCCP was added, all sperm in the population became immotile. The inability to undergo any significant respiration either disabled or killed the sperm.

4.2.2 Dog

Table 4.3 presents the results of dog sperm and Table 4.4 presents the statistical significance of the results. As a whole, the dog data had similar statistical results to the human data; there was no difference between any of the three groups' motility, and fluorescence displayed a similar increase and subsequent decrease when CCCP was added. Figure 4.2 shows the resulting box-plot for the three dog groups.

Dog sperm were incubated in no-glucose BWW media and prepared according to normal dog protocol. The untreated and dye-treated sperm had a VCL of 114.89 (n=130) and 113.41 (n=129), respectively. The CCCP + dye-treated sperm had a VCL of 90.75 (n=163), a clear drop in VCL from the other two groups. A second test was performed using a single wash and a double wash. The single wash and double wash sperm were both alive, with the no-glucose samples having much lower VCLs. Glucose-present media, single washed sperm had a VCL of 103.1 (n=21), while no-glucose media had a VCL of 48.2 (n=25) for single wash and 42.2 (n=25) for double wash. When CCCP was added to the samples, both single and double wash sperm experienced a loss of motility; the single wash had a very small amount of swimming sperm, and the double wash had no motile sperm. This indicates an effect of the washing protocol on glucose availability; human sperm undergo a double wash, dog sperm undergo a single wash. The single spin/wash leaves a higher chance that there will be remaining seminal fluid – and therefore the availability of glucose for the sperm can subsist on. This is seen in the first experiment, whereas the second experiment had a more effective washing protocol.

Table 4.3 shows the results of the three dog groups. The VCL and swimming force were on average higher than the human data and experienced little fluctuation in VCL and force.

	No Dye	Dye	CCCP + Dye
Dog VCL (μm/sec)	108.97 (n=334)	106.44 (n=472)	108.77 (n=370)
Dog Swimming Force (pN)	42.0 (n=104)	46.6 (n=116)	50.1 (n=54)
Dog Fluorescence Ratio (vs. No $DiOC_6(3)$)	-3.65×10^{-6} (n=100)	.192 (n=103)	.025 (n=53)

Table 4.4 shows that the difference between the VCL and swimming force for the three groups were insignificant. The fluorescence indicated expected significance due to the effect of the dye and then the CCCP.

	No Dye vs. Dye	No Dye vs. CCCP + Dye	Dye vs. CCCP + Dye
Dog VCL	0.06	0.18	0.33
Dog Swimming Force	0.39	0.27	0.73
Dog Fluorescence	**5.19×10^{-34}**	**9.33×10^{-15}**	**2.20×10^{-21}**

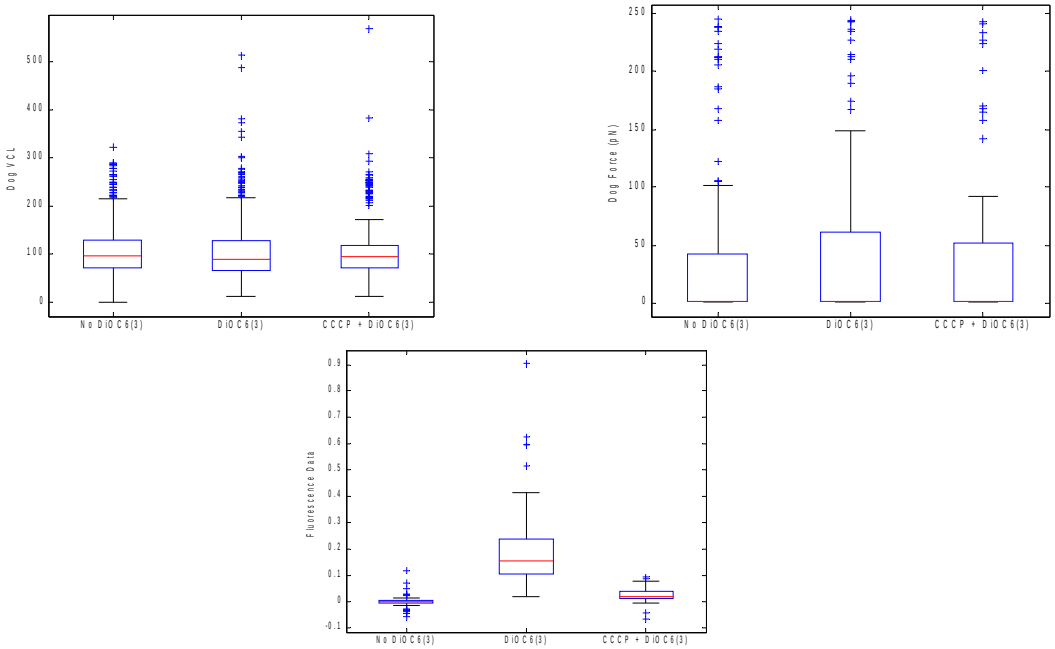

Figure 4.2: Boxplots for dog sperm. The boxplots show similar characteristics to the human boxplots. The VCL populations have a much higher number of outliers, but appear similar to each other.

4.2.3 Drill

Table 4.5 and 4.6 show the results for drill sperm. Drill sperm motility remained the same when $DiOC_6(3)$ was added, but experienced a decrease when CCCP was added. The swimming force appears to fluctuate considerably, but could be a result of a low sample size due to the difficulty of obtaining viable drill sperm samples. However, The decrease in VCL was statistically significant, and could indicate a reliance on both glycolysis and aerobic respiration for motility in this species. The fluorescence results were similar to the human and dog. Figure 4.3 shows the box-plots for the drill experiments. Appendix A.4 shows the data for low quality drill sperm that was not used for calculations in this thesis.

Table 4.5 shows the VCL, swimming force, and fluorescence ratio of drill sperm. The sperm exposed to the dye and CCCP experienced a drop in velocity. Fluorescence performed as expected.

	No Dye	Dye	CCCP + Dye
Drill VCL (μm/sec)	113.56 (n=256)	117.42 (n=280)	96.11 (n=162)
Drill Swimming Force (pN)	44.5 (n=17)	39.2 (n=16)	55.5 (n=35)
Drill Fluorescence Ratio (vs. No $DiOC_6(3)$)	-1.57×10^{-5} (n=277)	.62 (n=273)	2.69×10^{-2} (n=137)

Table 4.6 shows that the decrease in VCL seen in the CCCP+Dye group is statistically significant. The change in fluorescence for the no dye vs. dye and no dye vs. CCCP + dye showed significance as well, approaching the bottom limit of zero.

	No Dye vs. Dye	No Dye vs. CCCP + Dye	Dye vs. CCCP + Dye
Drill VCL	0.15	**8.27×10^{-11}**	**1.92×10^{-8}**
Drill Swimming Force	0.44	0.47	0.96
Drill Fluorescence	**0**	**0**	**2.69×10^{-60}**

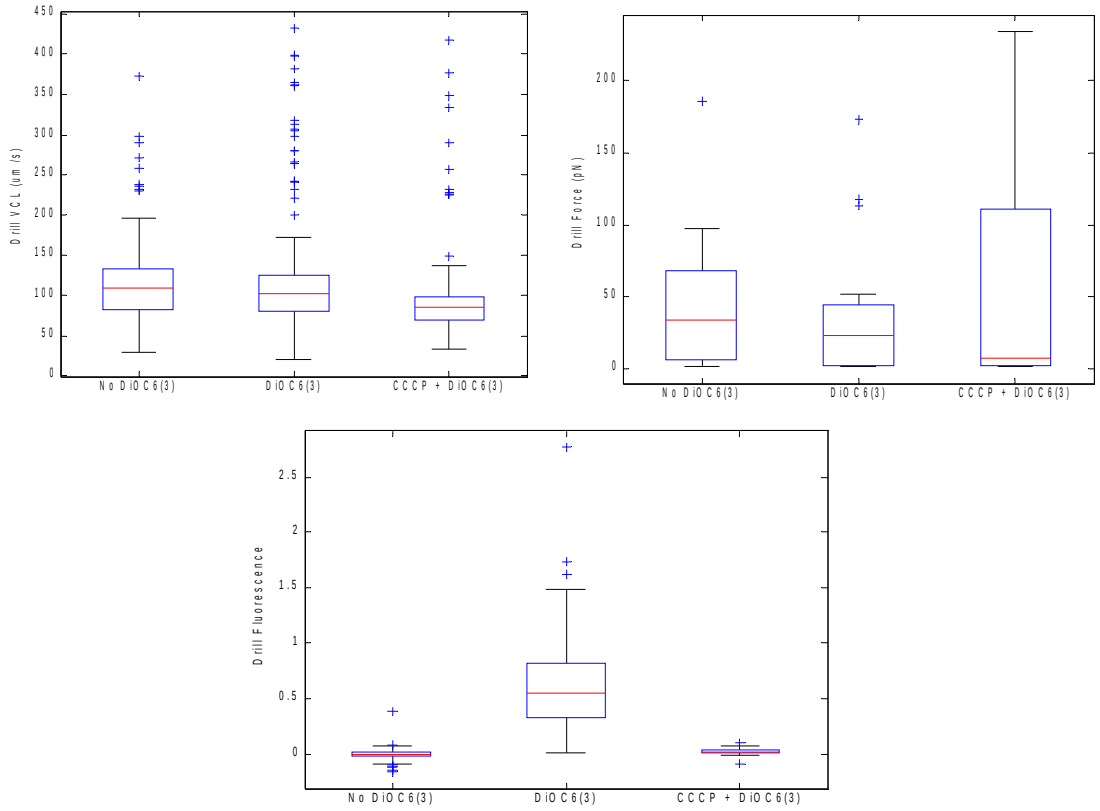

Figure 4.3 shows the box-plots of the drill sample. The drop in VCL seen in the above tables is also seen as a drop in the median in the box-plot. The low n-value for swimming force resulted in highly fluctuating values.

As a final test to determine a correlation between mitochondrial activity and motility, the fluorescence was plotted versus its respective velocity in human and drill samples (Figure 4.4). If higher VCL correlates with higher fluorescence, a relationship between VCL and fluorescence would be observable, but the data seems to be random. This would indicate that sperm motility is not reliant on mitochondrial midpiece activity. Removal of mitochondrial activity in drill resulted in lower VCL, so the lack of relationship between fluorescence and VCL may indicate that only a small amount of aerobic respiration is needed for the boost in VCL for drill.

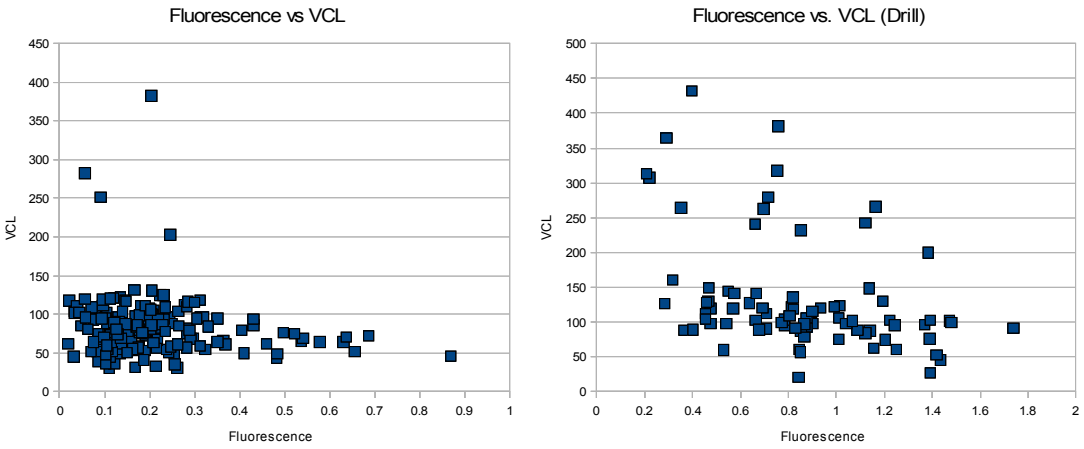

Figure 4.4 shows VCL vs Fluorescence ratio. There appears to be no correlation with membrane potential in the mitochondria and VCL.

Chapter IV, in part, is being prepared for submission for publication. Chen T., Shi L. Z., Zhu Q., Chandsawangbhuwana C., Berns M. W.

References

Donnelly E. T., Steele E. K., McClure N., Lewis S. E. M. (2001). Assessment of DNA integrity and morphology of ejaculated spermatozoa from fertile and infertile men before and after cryopreservation. *Human Reprod*. **16**(6), 1191-1199

V. Conclusions and Outlook

5.1 Conclusions

The purpose of this thesis was to investigate the effectiveness of $DiOC_6(3)$ as an indicator of mitochondrial activity and to use the dye to study the relationship between motility and aerobic respiration in sperm from several species (human, dog, and drill). The use of $DiOC_6(3)$ has proven to be effective at indicating whether or not there is significant aerobic respiration activity in sperm. It could be used to successfully stain the mitochondria (midpiece) in the three studied species as well as in mouse, and pig sperm (Appendix A) while having no effect on the sperm swimming speeds (VCL). The addition of the aerobic respiration inhibitor, CCCP, eliminated fluorescence in the three species of interest while having no effect on swimming force and varying effects on VCL. If aerobic respiration is the primary energy source for motility, it would be expected that the VCL would drop or be at zero if it was disabled. Since all the species are mammalian, it was expected that glycolysis would be the main source of motility and that CCCP inhibition would have a minimal effect. Human and dog sperm displayed the expected result of no force and VCL change with the dye added, and when the dye and the CCCP were added at the same time. Drill sperm experienced a decrease in VCL as aerobic respiration was inhibited, indicating a potential reliance on both glycolysis and aerobic respiration. The difference between the drill and the other two species was an unexpected finding, and bears further investigation.

As there have been very few studies on drill sperm, there could be a few reasons for its dependence on both glycolysis and aerobic respiration. Drills travel in variable-sized groups, ranging from 9, 93, or up to 400 (Gartlan 1970; Wild et al, 2005). This high degree of competition may select for stronger sperm that must generate energy from both ATP-producing processes. Drill sperm do indeed have a higher VCL and swimming force than dog or human sperm, both of which are not conventionally seen as competitive reproductively within their own species. Wild dogs travel in packs of only 4-8 adults (Woodroffe and Ginsberg, 1997) and humans are closer to a mating system with lower sperm competition (Martin 2007). Humans have some of the smallest midpieces amongst primates, indicating that activity in the midpieces is not nearly as important for sperm motility as in other species with larger midpieces. Larger midpiece volume have been correlated with multi-male systems (Anderson and Dixson, 2002), possibly due to the evolution of higher energy requirements because sperm from different males are competing to get to the egg. This idea requires further study, as other factors such as distance the sperm has to travel may play a role as well.

The successful performance of the non-ratiometric dye, $DiOC_6(3)$, confirms Nascimento's earlier results using a ratiometric dye (Nascimento, 2008). Since $DiOC_6(3)$ has shown to have no effect on sperm health, it is possible to integrate the use of different dyes or fluorescence markers to investigate sperm activity. $DiOC_2(3)$ requires the use of two emission wavelengths, while $DiOC_6(3)$ can utilize wavelengths outside of its emission range to investigate other dyes, such as calcium channel dyes. $DiOC_6(3)$ is effective as an indicator of respiration, but further studies regarding

whether the fluorescence intensity correlates with dye uptake are needed. Human sperm, with a smaller midpiece volume, would be predicted to have a lower fluorescence than the drill. Human sperm have a midpiece length of 7 um (Parastie), similar in length to dog sperm (Bartlett 1962) but shorter than the drill length of 15.6 um (Anderson et al, 2005). The results demonstrate that dog and human sperm have similar fluorescence, where the drill has a much higher fluorescence, perhaps reflecting the difference in midpiece size. Controls would need to be done to confirm that the difference is due to midpiece volume.

5.2 Future Directions

As discussed above, future experiments could study the relationship between midpiece volume, fluorescence intensity, and motility. This study could confirm the lack of relationship between VCL and fluorescence observed in the three species examined here. A greater midpiece volume, and therefore a posited higher fluorescence, should correlate with high motility in species completely reliant on aerobic respiration.

There are many other inhibitors available that can interrupt aerobic respiration or glycolysis in sperm. The observed decrease in drill sperm should be tested with other inhibitors to ensure that the result can be replicated with other drugs. If the conclusion is that glycolysis is the primary source of motility, the question becomes how do sperm swim when glucose is not present? Ch 1.2 discussed the idea of ATP shuttles or gluconeogenesis as possible candidates. Oxidative phosphorylation may convert present pyruvate into glucose to be used in glycolysis along the tail or in the

midpiece. If all the ATP is supplied from glycolysis in the midpiece, then the presence of ATP shuttles should be carefully studied. Adenylate kinase has been found in the flagella of sea urchin sperm (Su et al, 2005). Kinukawa has postulated that adenylate kinase may play a role in ATP regeneration for motilty, creatine rephosphorylation, or removing ADP (Kinukawa et al, 2007). A future study would be to inhibit adenylate kinase activity to investigate how that would affect motility. A potential inhibitor only recently used by Kinukawa, inhibits adenylate kinase without affecting oxidative phosphorylation (Lustorff and Schlimme, 1976).

A future project can also evaluate the sperm of species of different fertilization types. Species that undergo external fertilization and internal fertilization have very different sperm and mechanics. Eutherian species, such as marsupials, may provide an interesting link between the two fertilization types. Future motility and energetic studies may be useful in shedding light on sperm evolution and mating patterns.

Chapter V, in part, is being prepared for submission for publication. Chen T., Shi L. Z., Zhu Q., Chandsawangbhuwana C., Berns M. W.

References

Anderson M. J., Dixson A. F. (2002) Motility and the midpiece in primates. *Nature*. **416**, 496

Anderson M. J., Nyholt J., Dixson A. F. (2005). Sperm competition and the evolution of sperm midpiece volume in mammals. *J Zool, Lond*. 267, 135-142.

Bartlett D. J. (1962). Studies on dog semen. *J Reprod Fertil*. **3**, 173-189.

Gartlan J.S. (1970). Preliminary notes on the ecology and behavior of the drill, Mandrillus leucophaeus Ritgen, 1824. *In Old World Monkeys*. eds. J.R. Napier and P.H. Napier. Academic Press: New York. 445-480.

Kinukawa M., Nomura M., Vacquier V. D. (2007). A sea urchin sperm flagellar adenylate kinase with triplciated catalytic domains. *J of Biol Chem*. **282**, 2947-2955

Lustorff J., Schlimme E. (1976). Does an inhibitor of mitochondrial adenylate kinase also affect oxidative phosphorylation? *Cell and Mol Life Sciences*. **32**(3), 298-299

Martin R. D. (2007). The evolution of human reproduction: a primatological perspective. *Yearbook of Phys Anthro*. **50**, 59-84

Nascimento J. M., Shi L. Z., Tam J., Chandsawangbhuwana C., Durrant B., Botvinick E. L., Berns M. W. (2008). Comparison of glycolysis and oxidative phosphorylation as energy sources for mammalian sperm motility, using the combination of fluorescence imaging, laser tweezers, and real-time automated tracking and trapping. *J Cell Physiol* **217**, 745-751

Parastie S. (2008) The importance of sperm morphology in the evaluation of male infertility. 8th *Postgraduate Course for Training in Reproductive Medicine and Reproductive Biology*

Su Y. H., Chen S. H., Zhou H., and Vacquier V. D. (2005). Tandem mass spectrometry identifies proteins phosphorylated by cyclic AMP-dependent protein kinase when sea urchin sperm undergo the acrosome reaction. *Dev Biol*. **285**, 116–125

Wild C., Morgan B. J., Dixson A. (2005). Conservation of drill populations in Bakossiland, Cameroon: historical trends and current status. *Int J Primatol*. **26**(4):759-73.

Woodroffe R., Ginsberg J. R. (1997). Conserving the African wild dog Lycaon pictus. I. Diagnosing and treating the causes of decline. *Oryx*. **33**(2). 132-142.

Appendix: Effects of $DiOC_6(3)$ on Mice, Pig, and Drill Sperm

A.1 Introduction

This section outlines the experiments performed on mouse, pig, and some samples of drill sperm. The two animals were not pursued to a greater degree due to various problems with sperm quality and availability. The mouse sperm was often very immotile and with a short lifespan. The pig sperm could not be frozen, and therefore had to be ordered fresh commercially and tested with a special media. Pig sperm also was found to have a disk-like head morphology, making it difficult to trap, even at low VCLs. It was ultimately decided not to continue tests on these two species. The drill sperm ranged in quality depending on the speed of progression (SOP) before cryopreservation. The higher quality samples were used for the thesis, and the remaining samples are seen in this appendix.

A.2 Mouse

Mouse sperm was acquired from sacrificed mice, and the cauda was placed in buffer. The sperm was pushed out into the buffer, the tissue was removed, and the buffer was collected. The sperm health and count was evaluated using a hemacytometer, and used within the next couple hours. The sample was incubated in 50 nM of $DiOC_6(3)$.

The VCL, swimming force, and fluorescence for mouse was collected in Figure A.1. Mouse sperm differed greatly from the human, dog, or drill in preparation. Since mouse sperm was fresh, it was much more variable than the other species. The quality of a given sample was unknown, and often found to be very low quality or

immotile. Given the volatility of the samples, a high n-value could not be achieved for the CCCP+dye group. The high velocity in good samples made the sperm difficult to trap. Fluorescence from $DiOC_6(3)$ was observed, and was extinguished by the addition of CCCP in the small number of tests performed. Further experiments were not pursued due to repeated poor quality mouse sperm samples.

Table A.1. VCL, swimming force, and fluorescence ratio for mouse sperm. Mouse VCL was very fast, but the samples proved too unreliable to pursue in further studies.

	No Dye	Dye	CCCP + Dye
Mouse VCL (μm/sec)	156.07 (n=126)	138.6 (n=93)	125.7 (n=19)
Mouse Swimming Force (pN)	116.8 (n=16)	103.0 (n=15)	126.8(n=2)
Mouse Fluorescence Ratio (vs. No $DiOC_6(3)$)	$1.73x10^{-5}$ (n=70)	.16 (n=71)	.05 (n=10)

A.3 Pig

Pig sperm was received in Preserve Xtra extender media at 55ºF (supplied by Prairie State Semen). The sperm was thawed at 99-100ºF for 30 minutes, and diluted in BWW+BSA, since sterile Preserve Xtra extender was not available. The sample was loaded into a rose chamber and mounted onto the microscope. The sample was incubated in 50 nM of $DiOC_6(3)$ for 20 minutes.

Only one experiment was performed on the pig sperm. A fluorescent image of the sperm can be seen in Figure 3.5. Since the sperm was in BWW+BSA instead of Preserv Xtra extender, the population appeared sluggish. The VCL for undyed sperm was 83.38 (n = 52) and 81.53 (n = 11) for dye-treated sperm. Due to the need to order

special media, the relatively short shelf-life of the sperm, the sperm storage requirements, and cost it was decided not to continue tests on pig.

A.4 Drill

Drill sperm was prepared in the same manner as outlined in Chapter 3. Drill sperm fell into two categories: high and low quality. High quality sperm did not experience a noticeable decrease in VCL as time passed, had a higher percentage of motile sperm, and higher VCL. Experiments were performed simultaneously on the CASA system as the trapping experiments in order to confirm this. This sperm had SOPs of 3-4 (out of 5) before cryopreservation. Low quality sperm experienced a quick decrease in VCL within 30 minutes, had sparse population, and lower VCL. These samples had SOPs of 2-3 before cryopreservation.

Table A.2 shows the VCL, swimming force, and fluorescence for these drill samples. The low quality samples had much lower VCL and swimming force in all three of the categories of interest. Although high n-values, meaningful results cannot be deduced due to the deteriorating quality of the sperm over time and low percentage of live sperm per population. $DiOC_6(3)$ performed as expected, but to a lesser degree than what was seen in the high quality sperm. The fluorescence ratio was lower, but still indicated successful staining. CCCP managed to eliminate fluorescence.

Table A.2 shows the VCL, swimming force, and fluorescence for low quality drill sperm. The data was lower than good quality sperm and highly variable due to the volatility of the samples.

	No Dye	Dye	CCCP + Dye
Drill VCL (μm/sec)	77.48 (n=244)	57.69 (n=172)	70.00 (n=165)
Drill Swimming Force (pN)	22.05 (n=77)	40.39 (n= 57)	47.68 (n=51)
Drill Fluorescence Ratio (vs. No $DiOC_6(3)$)	$1.11x10^{-5}$ (n=62)	.26 (n=36)	.03 (n=44)